ORIGINAL ARTICLE

Comparative Analysis of Diffusion Tensor Imaging Estimation Methods

Somaye Jabari [1], Amin Ghodousian [1*], Reza Lashgari [2], Babak A. Ardekani [3]

[1] *Department of Algorithms and Computation, Faculty of Engineering Science, College of Engineering, University of Tehran, Tehran, Iran*

[2] *Institute of Medical Science and Technology, Shahid Beheshti University, Tehran, Iran*

[3] *Center for Advanced Brain Imaging and Neuromodulation, The Nathan S. Kline Institute for Psychiatric Research, Orangeburg, New York, USA*

*Corresponding Author: Amin Ghodousian
Email: a.ghodousian@ut.ac.ir

Received: 14 October 2024 / Accepted: 07 January 2025

Abstract

Purpose: Diffusion Tensor Imaging (DTI) is a noise-sensitive method, where a low Signal-to-Noise Ratio (SNR) results in significant errors in the estimated tensor field. This topic focuses on a comprehensive evaluation of various DTI estimation methods, such as Linear Least Squares (LLS), Weighted Linear Least Squares (WLLS), iterative re-weighted Linear Least Squares (IRLLS), and Non-linear Least Squares (NLS). The article will explore how each method performs in terms of accuracy, efficiency in estimating the diffusion tensor and robustness against noise.

Materials and Methods: The study compares the methods using simulated diffusion-weighted Magnetic Resonance Imaging (MRI) data. Time complexity and performance of the LLS, WLLS, IRLLS, and NLS methods were evaluated across key metrics such as TRMSE, RMSE, MSD, and ΔSNR.

Results: The results of the study demonstrate that LLS and IRLLS consistently outperform other methods in terms of TRMSE, MSD, and SNR, particularly in high-noise scenarios. NLS performs best in reducing RMSE but high noise causes it to fit to noise, so it is not robust. WLLS showed the weakest performance across all metrics.

Conclusion: The paper suggests that LLS, despite its simplicity, remains a competitive option in terms of capturing the true underlying diffusion properties. IRLLS further refines this by iteratively reducing the effect of outliers in tensor estimation.

Keywords: Diffusion Tensor Imaging; Diffusion Magnetic Resonance Imaging; Tensor Estimation Method; Cholesky Decomposition.

Copyright © 2026 Tehran University of Medical Sciences.
This work is licensed under a Creative Commons Attribution-NonCommercial 4.0 International license (https://creativecommons.org/licenses/by-nc/4.0/). Noncommercial uses of the work are permitted, provided the original work is properly cited.
DOI: https://doi.org/10.18502/fbt.v13i2.21943

Frontiers in BIOMEDICAL TECHNOLOGIES

1. Introduction

DTI is an advanced MRI technique that provides insights into the microstructural properties of tissues by measuring the diffusion of water molecules. In white matter, water diffusion is anisotropic, meaning it occurs more freely along the direction of aligned fibers, such as axons, and less freely across them. This directional dependence of diffusion is captured mathematically by a diffusion tensor, a second-order 3x3 matrix that describes the rate and direction of water movement in three-dimensional space. The tensor's eigenvalues and eigenvectors provide valuable metrics such as Fractional Anisotropy (FA) and Mean Diffusivity (MD), which are used to assess tissue integrity and connectivity. By estimating the diffusion tensor for each voxel in the brain, DTI enables detailed visualization and analysis of white matter pathways, playing a vital role in neuroscience, clinical diagnostics, and research.

DTI was introduced by Basser *et al.* in 1994 [1, 2]. In this method, diffusion in a voxel is represented by a second-rank tensor, which must be estimated for every voxel based on a series of Diffusion-Weighted MRI (DW-MRI) measurements [3-8], leading to an estimated tensor field. Diffusion tensor estimation involves various computational methods, each with its own strengths and limitations. LLS is a straightforward approach that uses ordinary linear regression after log-transforming the signal intensities [9]. It is simple and computationally efficient. WLLS tries to improve upon LLS by incorporating weights [7-10]. IRLLS further refines this approach by iteratively updating the weights to reduce the influence of outliers and improve accuracy. NLS avoids the need for a log transformation altogether, working directly with the nonlinear model. This allows NLS to make fewer assumptions about data uncertainty, albeit at the cost of increased computational complexity [8]. Each method strikes a different balance between accuracy, robustness, and efficiency, offering diverse options for diffusion tensor estimation. DTI has numerous applications across various fields, including neuroscience, clinical medicine, and research. Some key applications of DTI include mapping white matter tracts [11, 12], brain connectivity studies [13], neurological disorders [14, 15], stroke and traumatic brain injury [16-19], psychiatric disorders [20, 21], etc.

Since DTI has a wide range of applications, researchers in recent years have shown a tendency to use this method in new areas, while less emphasis has been placed on evaluating the performance of existing methods. We aim to compare LLS, WLLS, IRLLS, and NLS methods using new simulated dataset that closely resembles real brain structures and a Riemannian metric, which was not available when these methods were initially proposed. In this article, we delve into a detailed comparison of these DTI estimation methods, focusing on their accuracy, robustness to noise, and efficiency. In this context, accuracy refers to the extent to which the estimated diffusion tensor values reflect the true diffusion properties of the tissue. Computational efficiency refers to the ease of implementation and the computational time required. Robustness to noise indicates the resilience and reliability of a method under varying noise levels. To provide a comprehensive comparison, we employed a multi-faceted approach using simulated data. Simulated data, which mimics the complexities of real brain tissue, offers insights into how these methods handle realistic scenarios with varying noise levels while allowing us to compare results to the known ground truth.

The remaining sections of this paper are organized as follows. A brief description of the diffusion tensor is provided in Section 2.1. Approaches to estimate tensors, such as LLS, WLLS, IRLLS, NLS, and Cholesky decomposition, are outlined in Section 2.2. In Section 2.3, the time complexity of the mentioned methods is analyzed. The approach for calculating the distance between tensors is described in Section 3.1. In Section 3.2, the metrics used for comparing the methods are explained, followed by the simulated data and data analysis in Section 3.3. The results are presented in Section 4, while the discussion and conclusions are provided in Sections 5 and 6, respectively.

1.1. Diffusion Tensor

The diffusion tensor is a mathematical representation of the water diffusion process in three dimensions within a voxel. It describes the

relationship between the diffusion of water molecules within a voxel and the estimated diffusion tensor, which is central to understanding the microstructural properties of the tissue being imaged. In white matter, for example, the presence of myelinated axonal fibers constrains the movement of water molecules, allowing them to diffuse more freely along the length of the fibers (axial diffusion) and less freely across them (radial diffusion).

DTI assumes that the diffusion of water molecules follows a Gaussian probability density function within each voxel [1, 22] (Equation 1):

$$\rho(x|x_0,\tau) = \frac{1}{\sqrt{(4\pi\tau)^3|D|}}\, exp\left[-\frac{(x-x_0)^T D^{-1}(x-x_0)}{4\tau}\right] \quad (1)$$

The function expresses the probability that a water molecule, initially at x_0 at time 0, reaches position x at time τ. Here, D, the diffusion tensor, describes the molecules displacement. The displacement is supposed to be uniform within the voxel.

D represents a covariance matrix which is a 3 × 3 symmetric positive definite (SPD) matrix. We denote the set of m × m SPD matrices by $\mathcal{S}_m^+$, so $D \in \mathcal{S}_3^+$ describes how diffusion varies along different directions within the voxel (Equation 2).

$$D = \begin{bmatrix} D_{xx} & D_{xy} & D_{xz} \\ D_{xy} & D_{yy} & D_{yz} \\ D_{xz} & D_{yz} & D_{zz} \end{bmatrix} \quad (2)$$

Where D_{xx}, D_{yy}, D_{zz} are the diffusion coefficients along the principal axes and D_{xy}, D_{yz}, D_{xz} are the diffusion coefficients that describe the coupling between different directions. This assumption simplifies the modeling and allows the diffusion process to be described by the diffusion tensor [23].

1.2. Tensor Estimation

The relationship between the measured DW-MRI signal and the diffusion tensor is described by the Stejskal-Tanner model [22] (Equation 3):

$$S_i(D,S_0) = S_0\, exp(-b_i g_i^T D g_i) \quad (3)$$

Where $S_i(D,S_0)$ is a predictor of the DW-MRI signal measured in terms of a known direction of the diffusion sensitizing field gradient , represented by a unit vector $g_i \in \mathbb{R}^3$, a known scalar $b_i \in \mathbb{R}^+(s/mm^2)$ representing the strength and timing of the diffusion sensitizing field gradient, an unknown reference T2-weighted signal, $S_0 \in \mathbb{R}^+$, denoting the image intensity in the absence of diffusion sensitizing (i.e., when $b_i = 0$), and an unknown SPD matrix (mm^2/s).

In the absence of noise, $S_i(D,S_0) = y_i$ is established. However, Noise introduces a discrepancy between the predicted and the measured signal that usually called error (ε): $S_i(D,S_0) = y_i + \varepsilon_i$. Given a sequence of DW-MRI measurements, $y_i\ (i = 1,2,\ldots,n)$, with varying b_i and g_i, the objective of DTI analysis is to estimate a diffusion tensor D and a baseline signal level S_0 for each voxel to minimize the error. This is achieved by defining and minimizing a cost as a function of D and S_0 [8]. One common approach is to use the least square error (Equation 4):

$$J_{NLS}(D,S_0) = \frac{1}{2}\sum_{i=1}^{n}(y_i - S_i(D,S_0))^2 \quad (4)$$

It is called the NLS method because (Equation 3) is not linear.

While NLS typically works directly with the non-linear model, sometimes the logarithmic transformation of (Equation 3) is used (Equation 5):

$$J_{LLS}(D,S_0) = \frac{1}{2}\sum_{i=1}^{n}(\ln y_i - \ln S_i(D,S_0))^2 \quad (5)$$

It is called LLS. This method is computationally efficient and serves as a good starting point for more complex methods.

The WLLS method assigns weights to (Equation 6):

$$J_{WLLS}(D,S_0) = \frac{1}{2}\sum_{i=1}^{n}\omega_i^2(\ln y_i - \ln S_i(D,S_0))^2 \quad (6)$$

The optimal weight is the measured signal [7, 8]. The implementation of these methods is thoroughly explained in [8]. The IRLLS repeatedly applies a WLLS procedure, where the weights are updated in each iteration [24]. This method aims to reduce the influence of outliers.

To ensure the estimated tensor is an SPD matrix, some constraints must be enforced on the tensor estimation methods. Using Cholesky decomposition, we can ensure that the estimated tensor is positive definite [25, 26]. Let $\mathcal{L}_m$ denote the set of all $m \times m$ lower-triangular matrices and $\mathcal{L}_m^+$ denote the subset of $\mathcal{L}_m$ with strictly positive diagonal elements. The Cholesky decomposition assigns to every $A \in \mathcal{S}_m^+$ a unique $L \in \mathcal{L}_m^+$ such that (Equation 7):

$$A = LL^T \tag{7}$$

Recalling the Cholesky decomposition to enforce positivity on the estimated diffusion tensor, we rewrite (Equation 3) as a function of the unconstrained $L \in \mathcal{L}_m^+$ as follows (Equation 8):

$$S_i(L, S_0) = S_0 \, exp(-b_i g_i^T LL^T g_i) \tag{8}$$

The least square algorithms are reformulated according to (Equation 8). For example, the NLS algorithm in (Equation 4) is replaced by (Equation 9):

$$J_{CNLS}(L, S_0) = \frac{1}{2}\sum_{i=1}^{n}(y_i - S_i(L, S_0))^2 \tag{9}$$

We refer to this method as constraint non-linear least squares (CNLS). In this way, we will have constraint linear least squares (CLLS), constraint weighted linear least squares (CWLLS) and constraint iterated re-weighted linear least squares (CIRLLS). Note that these constrained least squares problems are no longer linear because $\ln S_i(L, S_0)$ is not a linear function of L. The constrained methods are only applied when the tensor estimated using unconstrained methods is not SPD.

1.3. Time Complexity

The time complexity of an algorithm refers to the computational cost relative to the size of the input data. Grasping the time complexity of tensor estimation methods is crucial to assess their practicality in various research and clinical contexts, particularly when working with large datasets or requiring real-time processing. Time complexity evaluates how long an algorithm takes to execute, depending on the input size, typically denoted as $T(n)$ for an input size of n. It serves as a measure of the algorithm's efficiency. To analyze an algorithm's time complexity, the objective is to count the number of basic operations it performs as the input size grows. These basic operations are simple steps, like adding two numbers, which take a fixed amount of time regardless of input size.

To analyze the time complexity of the LLS, WLLS, IWLLS, and NLS methods, we make the following assumptions: these methods operate on a point-wise basis, and the calculations are uniform across all brain voxels. Therefore, we calculate the time complexity for a single voxel, which will apply to all of them. Each method involves several matrix operations. For simplicity, we assume that all matrices are of size $n \times n$ and vectors have a dimension of size n, solely for the purpose of time complexity calculation. We suppose n is the number of DW-MRI measurements. For matrix multiplication, although more efficient algorithms exist (such as the Strassen's algorithm which has a complexity of $\left(n^{log_2^7}\right)$ [27]), we use the standard matrix multiplication algorithm with a time complexity of (n^3). The matrix inversion process also has a time complexity of (n^3) when using the Gaussian elimination method. Additionally, matrix transposition and Jacobian matrix computation both have a time complexity of (n^3).

To estimate tensors by linear methods, LLS, WLLS, and IRLLS, the numerical approaches, including the normal equations method, are employed. The time complexity of LLS using normal equations is $T_{LLS}(n) = 4n^3 + n^2$ (three matrix multiplications, one matrix inversion and one matrix transpose). Similarly, $T_{WLLS}(n) = 6n^3 + n^2$ (five matrix multiplications, one matrix inversion and one matrix transpose). For IRLLS, there are m_I iterations and each iteration has the same time complexity as WLLS. Therefore, the time complexity is given by $T_{WLLS}(n) = m_I\,(6n^3 + n^2)$. In our implementation, we selected $m_I = 3$.

The NLS optimization problem is solved iteratively using numerical methods such as the Gauss-Newton and Levenberg-Marquardt algorithms. These methods require an initial estimate to initiate the optimization process. In the case of DTI, the initial guess for the tensors can be obtained from tensor estimates derived using linear methods. The number of iterations in these algorithms is not predefined; however, in our implementation, we set the maximum number of

iterations to 100. To approximate the time complexity of NLS, we focus on the Gauss-Newton method. At each iteration, the following equation must be solved (Equation 10):

$$X^{(k+1)} = X^{(k)} - (J^T J)^{-1} J^T S(X^{(k)}) \quad (10)$$

Where $X^{(k)}$ represents the solution at iteration k, $X^{(k+1)}$ is the updated solution at iteration $k + 1$ and J is the Jacobian matrix of $S(X^{(k)})$. For each iteration, the complexity time is approximated as $4n^3 + 2n^2$. Assuming m_N iteration, the complexity time of NLS is $T_{NLS}(n) = m_N\,(4n^3 + 2n^2)$. This estimation does not include the time complexity of the initial guess computation.

2. Materials and Methods

2.1. Log-Cholesky Distance

To compare tensors, we need suitable metric between SPD matrices. In the context of DTI, previous studies have regarded the space of SPD matrices $\mathcal{S}_m^+$ as a Riemannian manifold. A Riemannian manifold is a type of smooth manifold equipped with a Riemannian metric, which allows for the definition of geometric concepts like distances, angles, and volumes on the manifold. The Riemannian metric gives a way to measure the distance between points on the manifold. Previously utilized metrics for this purpose are the Frobenius [28], the affine-invariant (Fisher) [29, 30], and the Log-Euclidean [31-33] metrics. The Log-Cholesky metric has been introduced recently [34] as an alternative with several advantages, including computational efficiency, no swelling effect, a closed-form formula for averaging, and parallel transport along the geodesic. We decide to use the Log-Cholesky metric to calculate the distance between tensors.

The Log-Cholesky Riemannian metric uses Cholesky decomposition. Suppose $D_1, D_2 \in \mathcal{S}_m^+$ and $d^2_{\mathcal{S}^+}(D_1, D_2)$ be the distance between D_1 and D_2. Let $L_1, L_2 \in \mathcal{L}_m^+$ be the Cholesky decomposition of D_1, D_2, respectively, and $d^2_{\mathcal{L}^+}(L_1, L_2)$ be the Log-Cholesky distance between L_1 and L_2. $d^2_{\mathcal{L}^+}(L_1, L_2)$ is defined like this (Equation 11):

$$d^2_{\mathcal{L}^+}(L_1, L_2) = \| \mathbb{L}(L_1) - \mathbb{L}(L_2) \|_F^2 + \| \log \mathbb{D}(L_1) - \log \mathbb{D}(L_2) \|_F^2 \quad (11)$$

That $\mathbb{L}(L_1)$ denotes the strictly lower-triangular part of L_1, $\mathbb{D}(L_1)$ denotes the diagonal part of L_1. For matrix $A_{m\times n}$ (Equation 12):

$$\| A \|_F^2 = \sum_{i=1}^{n}\sum_{j=1}^{m} A_{ij}^2 \quad (12)$$

Finally $d^2_{\mathcal{S}^+}(D_1, D_2)$ is defined like this (Equation 13):

$$d^2_{\mathcal{S}^+}(D_1, D_2) = d^2_{\mathcal{L}^+}(L_1, L_2) \quad (13)$$

2.2. Metrics

For simulated, we can have noise-free signals that by using any tensor estimation method, we will have the origin tensor field. In this section, some quantitative metrics are presented for comparison between the methods using the noise-free signals and the origin tensor field. In the following, $S_i(v)$ is the noise-free DW-MRI, $\tilde{S}_i(v)$ is the noisy DW-MRI, and $\hat{S}_i(v)$ is the estimated DW-MRI, all at voxel v. The number of diffusion-sensitizing gradient directions is n, N is the number of voxels, and v denotes the voxel coordinates.

TRMSE: We also calculated the voxel-wise true root mean squared error (TRMSE) between the noise-free DW-MRI signals S_i and estimated DW-MRI signals $\hat{S}_i$ for all voxels as follows (Equation 14):

$$TRMSE = \frac{1}{N}\sum_{v}\sqrt{\frac{1}{n}\sum_{i=1}^{n}\left(\hat{S}_i(v) - S_i(v)\right)^2} \quad (14)$$

RMSE: We calculated the mean of the voxel-wise root mean squared error (RMSE) between the noisy DW-MRI signals $\tilde{S}_i$ and estimated DW-MRI signals $\hat{S}_i$ averaged over all voxels as follows (Equation 15):

$$RMSE = \frac{1}{N}\sum_{v}\sqrt{\frac{1}{n}\sum_{i=1}^{n}\left(\hat{S}_i(v) - \tilde{S}_i(v)\right)^2} \quad (15)$$

MSD: The mean squared distance (MSD) is a metric between the origin tensor (D) and the estimated tensor ($\widehat{D}$) averaged over all voxels that is calculated as (Equation 16):

$$MSD = \frac{1}{N}\sum_{v} d_{S^+}^2\left(D(v), \widehat{D}(v)\right) \qquad (16)$$

That d_{S^+} is the Log-Cholesky distance given by (Equation 12).

ΔSNR: Another quantity is ΔSNR (signal-to-noise rate) computed as follows (Equation 17):

$$\Delta SNR = 10\log\left(\frac{\sum_v \sum_{i=1}^{n}\left(\tilde{S}_i(v) - S_i(v)\right)^2}{\sum_v \sum_{i=1}^{n}\left(\hat{S}_i(v) - S_i(v)\right)^2}\right) \qquad (17)$$

2.3. Simulated Data and Data Analysis

We used simulated DW-MRI to compare the LLS, WLLS, IRLLS, and NLS estimations. Simulated DW-MRI generated 3 data called 1st, 2nd, and 3rd data using ExploreDTI software on matrices of 79 × 107 × 60 voxels. 1st data has 32 directions with 2 images at b = 0 and 30 at b = 1000 s/mm^2. 2nd data has 66 directions with 6 images at b = 0 and 60 at b = 1200 s/mm^2, and 3rd data has 30 directions with 5 images at b = 0 and 25 at b = 2000 s/mm^2. Simulated data were created at five SNR levels: SNR = 5, 10, 15, 25, and SNR = ∞ (noise-free). The tensor field estimated from noise-free signals using the CLLS method is considered as the reference (or origin) tensor field.

To evaluate DTI applications and highlight their importance, we aim to compare the results of DTI reconstruction methods. In this paper, we specifically compare the results of the LLS, WLLS, IRLLS, and NLS methods. For all methods, when the estimated tensor is not SPD, the constrained method is used. The implementation of these methods is based on the description provided in [8]. All methods were implemented in Python. The tools MRTrix [35], Camino [36], ParaView [37], and ExploreDTI [38] were employed for visualization.

3. Results

Table 1 presents a comparison of the methods using TRMSE, RMSE, MSD, and ΔSNR metrics applied to the 1st, 2nd, and 3rd simulated datasets. The results in the table show that the LLS and IRLLS methods performed best in TRMSE, MSD, and ΔSNR at all SNR levels. Conversely, NLS excelled in RMSE across all SNR levels. The RMSE, which measures the discrepancy between noisy and estimated signals, is defined similarly to the NLS cost function (Equation 9). While non-linear methods minimize the cost function effectively, the results demonstrate that they do not necessarily provide the best tensor estimation. Interestingly, the WLLS method consistently underperformed across all metrics. Its weighting scheme, designed to mitigate noise, appeared ineffective for this dataset, resulting in poorer outcomes than the simpler LLS or the more advanced NLS. Figure 1 illustrates voxel-wise histograms of the TRMSE and MSD at SNR=5 and 15.

Figure 2 depicts the estimated tensor fields obtained using the LLS, WLLS, IRLLS, and NLS methods. Sections of the brain in the axial view are shown. Qualitatively, the figure indicates that at high SNR levels, all methods yield similar estimations, whereas at low SNR levels, the WLLS method performs worse than the others.

Tractography was performed on the tensor field estimated using CLLS, CWLLS, CIRLLS, and CNLS as generated by the Camino package [36] and is shown in Figure 3. The results show that the WLLS method produced fewer tracts at all SNR levels.

4. Discussion

DTI has revolutionized our understanding of the brain's structural connectivity and has become instrumental in both clinical and research settings. Clinically, it aids in the diagnosis and management of neurological disorders such as multiple sclerosis, stroke, and traumatic brain injury by highlighting abnormalities in white matter tracts. In research, DTI provides invaluable data for studying brain development, aging, and the effects of various neurodegenerative diseases.

Table 1. The results of the methods on the 1st, 2nd, and 3rd simulated data

SNR	metric	LLS				WLLS				IRLLS				NLS			
		1st	2nd	3rd	Avg.	1st	2nd	3rd	Avg.	1st	2nd	3rd	Avg.	1st	2nd	3rd	Avg
5	TRMSE	142	110	184	145	270	272	314	285	155	119	190	154	164	145	221	176
	RMSE	232	243	208	227	258	275	234	255	227	241	204	224	225	231	194	216
	MSD	0.40	0.29	0.51	0.4	0.62	0.84	0.72	0.72	0.40	0.40	0.51	0.43	0.40	0.36	0.59	0.45
	ΔSNR	5.5	7.5	3.9	5.6	0.5	0.01	-0.5	0.0	5.4	6.3	3.6	5.1	4.4	5.2	2.4	4
10	TRMSE	69	50	79	66	99	98	132	109	67	50	78	65	69	55	88	70
	RMSE	124	132	113	123	133	142	126	133	123	131	111	121	120	129	108	119
	MSD	0.19	0.13	0.21	0.17	0.25	0.22	0.33	0.26	0.18	0.13	0.21	0.17	0.18	0.13	0.23	0.18
	ΔSNR	5.8	8.5	4.8	6.3	2.5	2.8	0.4	1.9	6.0	8.0	4.8	6.2	5.7	7.7	3.8	5.7
15	TRMSE	45	33	51	43	58	53	77	62	44	33	50	42	45	34	53	44
	RMSE	84	89	79	84	88	94	86	89	83	89	78	83	83	88	76	82
	MSD	0.12	0.08	0.14	0.11	0.14	0.11	0.20	0.15	0.12	0.08	0.13	0.11	0.12	0.08	0.14	0.11
	ΔSNR	6.1	8.8	5.0	6.6	3.9	4.6	1.5	3.3	6.2	8.2	5.1	6.5	6.1	8.4	4.5	6.3
25	TRMSE	27	19	30	25	30	25	39	31	26	19	29	24	26	19	30	25
	RMSE	51	54	49	51	52	55	52	53	50	54	48	50	50	53	48	50
	MSD	0.07	0.05	0.08	0.06	0.07	0.06	0.1	0.07	0.07	0.05	0.08	0.06	0.07	0.06	0.08	0.07
	ΔSNR	6.2	9.0	5.2	6.8	5.2	6.6	2.9	4.9	6.4	8.7	5.4	6.8	6.3	8.8	5.2	6.7

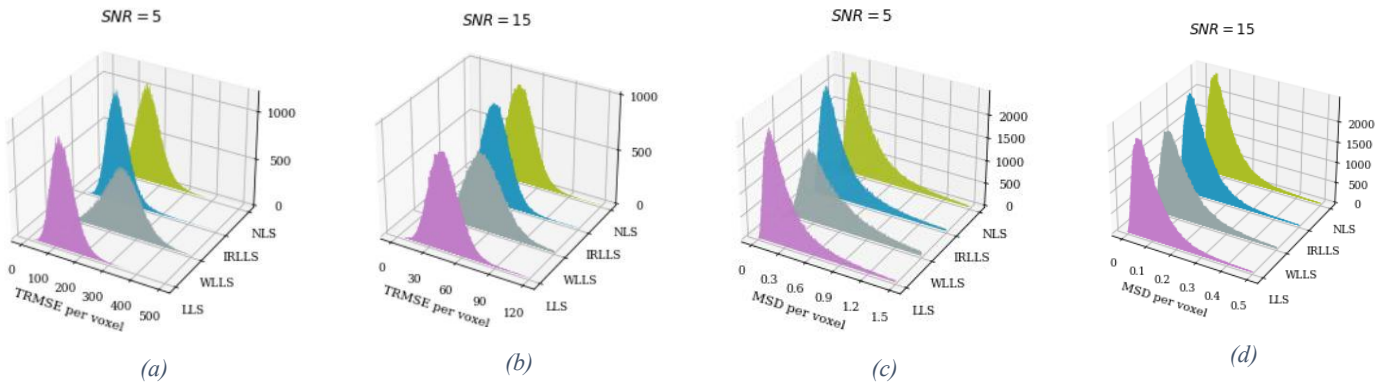


Figure 1. The plots show the voxel-wise histogram of the TRMSE (panel (a),(b)) and the MSD (panel (c),(d)) of LLS, WLLS, IRLLS, and NLS methods

There is ongoing debate regarding the use of linear methods in DTI analysis. Some argue that these methods distort the variance of DW signals due to logarithmic transformation, thereby violating the uniform variance (homoscedasticity) assumption required by LLS [1, 39]. Simulations conducted in [1] reveal that NLLS produces the most accurate estimates, followed by WLLS and then LLS, particularly under noisy conditions. These studies suggest that nonlinear methods should be preferred and explicitly recommend that, if linear methods are used, at a minimum, the WLLS method should be applied [1, 8, 39].

In contrast, some argue that if the weighted signal follows a Rician distribution and SNR>2, and then the log-transformation ensures that the expected error becomes zero, resulting in an unbiased estimation [7, 10]. Theoretically, there are many reasons that may lead to the violation of the two aforementioned conditions for the DW signal, one of which is the use of preprocessing methods. In such cases, it can be argued that linear estimation is biased. However, practical results have shown that LLS achieves higher accuracy compared to NLS. It should be noted that achieving higher accuracy, alongside the simplicity of the method, is highly important. Many methods have been proposed to enhance accuracy, but due to their high complexity, they have rarely been used in practice [40].

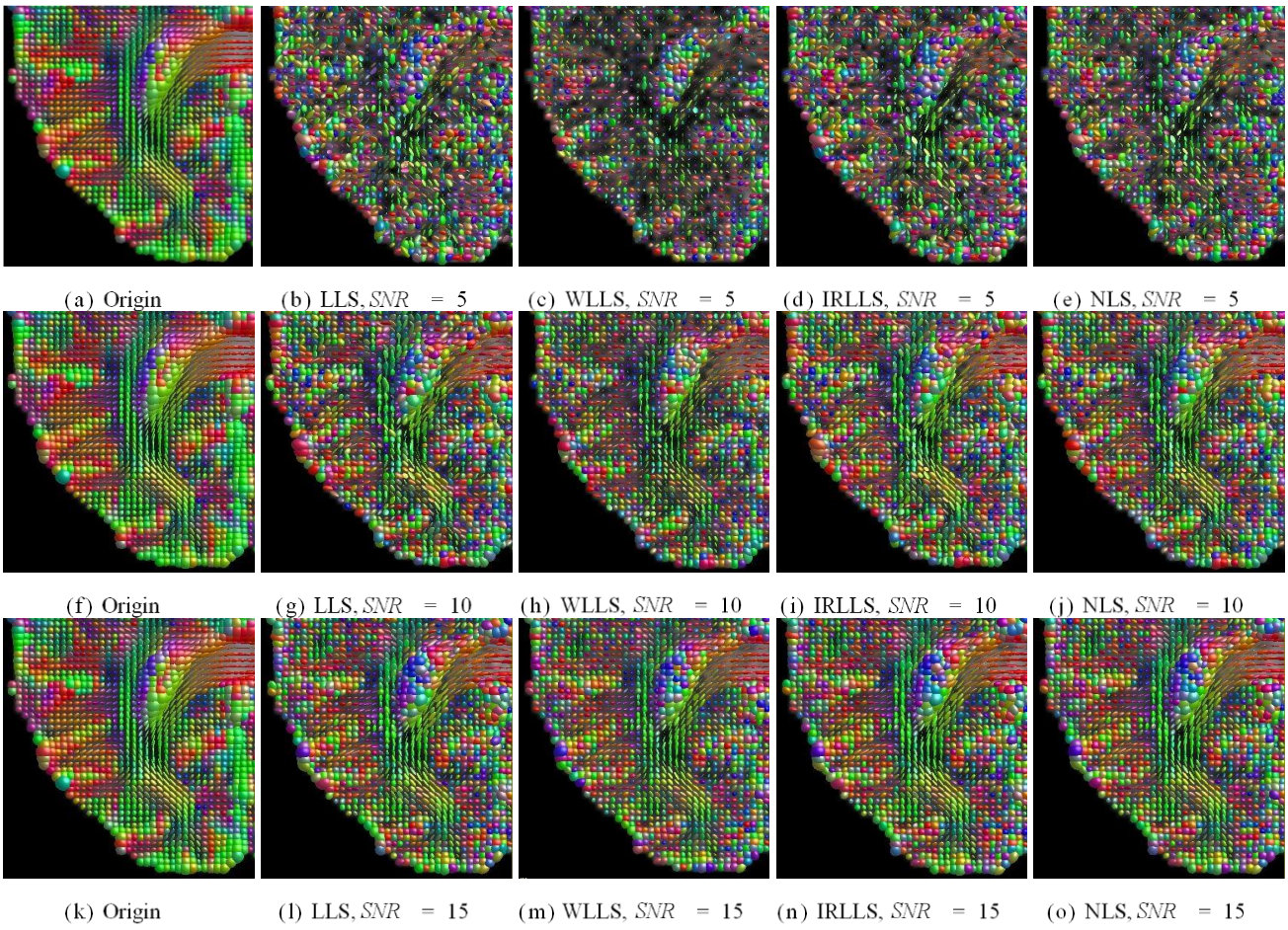


Figure 2. The images show the axial view of the simulated brain by the LLS, WLLS, IRLLS, and NLS methods at three SNR levels: SNR = 5,10,15

The use of weighting for linear methods has been suggested since the initial introduction of DTI, where the square of the DW signal, which is also noisy, is used as the weight. Many existing software tools utilize this approach for WLLS [10]. After some time, the stepwise weighting method was introduced that we called IRLLS, in which the weight is the square of the estimated signal. This method also acts as an outlier detection technique and has been shown to be one of the best methods for tensor estimation [22].

We decided to compare the LLS, WLLS, IRLLS, and NLS methods using simulated data across different SNR levels. To address some of the practical limitations of these methods, constrained versions of LLS, WLLS, IRLLS, and NLS referred to as CLLS, CWLLS, CIRLLS, and CNLS were developed. These constrained approaches enforce the positive definite condition on the estimated diffusion tensors, ensuring that the physical properties of diffusion are respected (i.e., the estimated diffusion tensors yield only positive eigenvalues). This constraint is particularly useful in regions with crossing fibers or low signal intensity, where unconstrained methods might produce physically unrealistic tensors. The use of Cholesky decomposition in these methods guarantees that the resulting tensors are positive definite.

The TRMSE, MSD, and ΔSNR metrics at different SNR levels indicate that LLS and IRLLS outperform other methods in terms of true error reduction and maintaining tensor accuracy and robustness at all SNR levels. This suggests that, despite its simplicity, LLS remains a competitive option for capturing the true underlying diffusion properties. IRLLS further refines this by iteratively reducing the effect of outliers. The NLS method performed poorly only at the low SNR level (SNR = 5), indicating that it is not robust. The WLLS method, however, performed poorly across all noise levels.

We have evaluated the methods in terms of computational time. LLS is the most efficient. The time complexity of WLS is slightly more than LLS. IRLLS runs m_I (m_I is fixed) iteration for all voxels. Usually, m_I

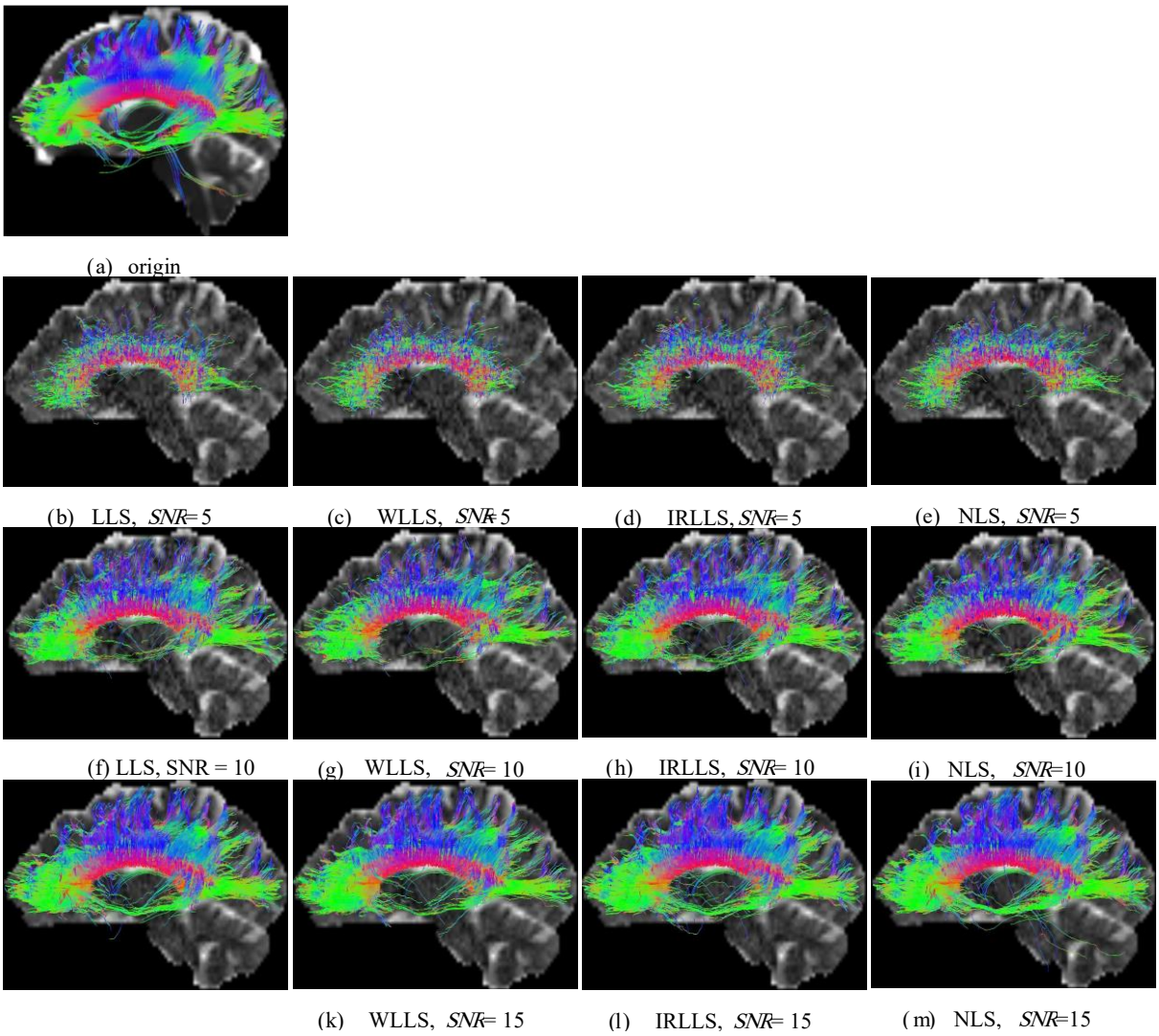


Figure 3. Tractography on noise-free (origin, panel (a)) and tensor field estimates by the LLS method (panels (b), (f), (j)), the WLLS method (panels (c), (g), (k)), the IRLLS method (panels (d), (h), (l)), and the NLS method (panels (e), (i), (m)) using 1st simulated brain DW-MRI data at SNR = 5 (second row), SNR = 10 (third row), and SNR = 15 (forth row)

is less than 5 and each iteration has the complexity time of WLS. The implementation of LLS, WLS, and IRLLS is simple by using standard matrix operations.

NLS operates directly on the nonlinear diffusion model, using iterative optimization algorithms like Gauss-Newton or Levenberg-Marquardt. Using the Gauss-Newton method, the time complexity of each iteration is near the LLS time complexity. Since NLS requires many iterations to converge, the overall time complexity increases significantly with the number of iterations. Also, NLS needs initial estimation to start. These cause NLS to be the most computationally expensive method.

5. Conclusion

This study provides a comprehensive comparison of various DTI estimation methods. We present a detailed comparative analysis of the efficiency, accuracy, and robustness of LLS, WLLS, IRLLS, and NLS methods, highlighting their performance across several critical metrics, including TRMSE, RMSE, MSD, and ΔSNR.

LLS offers excellent accuracy, computational efficiency, and robustness, making it suitable for routine DTI analyses. IRLLS stands out for its robustness against outliers, offering a balance between computational efficiency and improved performance in complex regions. WLLS, however, emerges as the weakest

method, performing poorly across all metrics and failing to reconstruct tracts effectively. NLS, while computationally expensive, demonstrates good accuracy at high SNR levels but lacks robustness to noise due to fitting to noise.

It is important to note that the presented results analyzed all brain voxels uniformly. For future research, the explored methods could be analyzed in key regions of interest, such as the corpus callosum, corticospinal tract, or hippocampus.

Ultimately, we hope the findings of this study provide valuable guidance for researchers and clinicians in selecting the most appropriate DTI estimation method.

Acknowledgment

The authors would like to sincerely thank the National Brain Mapping Lab for their valuable support and contributions to this research.

References

1- P. J. Basser, "MR diffusion tensor spectroscopy and imaging." *Biophys,* Vol. 66pp. 259-67, (1994).

2- J. Mattiello P. Basser, and D. LeBihan, "Estimation of the effective self-diffusion tensor from the NMR spin echo." *Journal of Magnetic Resonance,* Vol. 103pp. 247-54, (1994).

3- P. J. Basser, "Inferring microstructural features and the physiological state of tissues from diffusion-weighted images." *NMR Biomedicine,* Vol. 8pp. 333–44, (1995).

4- D. L. Bihan, "Diffusion tensor imaging: Concepts and applications." *Journal of Magnetic Resonance Imaging,* (2001).

5- P. J. Basser, "Microstructural and physiological features of tissues elucidated by quantitative-diffusion-tensor." *Journal of Magnetic Resonance,* Vol. 111pp. 209-19, (1996).

6- P. J. Basser, "Diffusion-tensor MRI: theory, experimental design and data analysis - a technical review." *NMR in Biomedicine,* Vol. 15pp. 456–67, (2002).

7- R. Salvador, A. Pena, D. K. Menon, T. A. Carpenter, J. D. Pickard, and E. T. Bullmore, "Formal characterization and extension of the linearized diffusion tensor model." *Hum Brain Mapp,* Vol. 24 (No. 2), pp. 144-55, Feb (2005).

8- C. G. Koay, L. C. Chang, J. D. Carew, C. Pierpaoli, and P. J. Basser, "A unifying theoretical and algorithmic framework for least squares methods of estimation in diffusion tensor imaging." *J Magn Reson,* Vol. 182 (No. 1), pp. 115-25, Sep (2006).

9- C. G. Koay, "Least squares approaches to diffusion tensor estimation." in *Diffusion MRI*, D. Jones, Ed. New York: *Oxford University Press*, (2011), pp. 281-343.

10- Veraart J., "Weighted linear least squares estimation of diffusion MRI parameters: strengths, limitations, and pitfalls." *NeuroImage* pp. 335-46, (2013).

11- P. G. Nucifora, "Diffusion-tensor MR imaging and tractography: exploring brain microstructure and connectivity." *Radiology,* Vol. 2pp. 367-84, (2007).

12- A. Faria K. Oishi, P. van Zijl, and S. Mori, MRI Atlas of Human White Matter. *Elsevier Science*, (2010).

13- E. W. Lang, "Brain connectivity analysis: A short survey." *Computational Intelligence and Neuroscience,* Vol. 1(2012).

14- B. Bodini and O. Ciccarelli, "Diffusion MRI in neurological disorders." in *Diffusion MRI*: *Academic Press*, (2014), pp. 241-55.

15- T. Woo-Suk, "Current clinical applications of diffusion-tensor imaging in neurological disorders." *Journal of Clinical Neurology* (2018).

16- C. Cavaliere, "Diffusion tensor imaging and white matter abnormalities in patients with disorders of consciousness." *Frontiers in Human Neuroscience,* Vol. 8(2015).

17- M. Georgios, "Traumatic brain injuries and diffusion tensor imaging a review." *Recent Patents on Medical Imaging,* Vol. 2pp. 36-50, (2012).

18- D. B. Douglas, "Diffusion Tensor Imaging of TBI: Potentials and Challenges." *Topics in magnetic resonance imaging : TMRI,* pp. 241-51, (2015).

19- S. H. Jang, "Role of Diffusion Tensor Imaging in the Diagnosis of Traumatic Axonal Injury in Individual Patients with a Concussion or Mild Traumatic Brain Injury: A Mini-Review." *Diagnostics,* (2022).

20- O. Abe T. Shizukuishi, "Diffusion tensor imaging analysis for psychiatric disorders." *Magnetic resonance in medical sciences : MRMS* pp. 153-59, (2013).

21- T. White, "Diffusion tensor imaging in psychiatric disorders." *Topics in magnetic resonance imaging: TMRI,* pp. 97-109, (2008).

22- E. O. Stejskal and J. E. Tanner, "Spin Diffusion Measurements: Spin Echoes in the Presence of a Time-Dependent Field Gradient." *The Journal of Chemical Physics,* Vol. 42 (No. 1), pp. 288-92, (1965).

23- A. L. Alexander, "A geometric analysis of diffusion tensor measurements of the human brain." *Magnetic Resonance in Medicine,* pp. 283-91, (2000).

24- Q. Collier, J. Veraart, B. Jeurissen, A. J. den Dekker, and J. Sijbers, "Iterative reweighted linear least squares

for accurate, fast, and robust estimation of diffusion magnetic resonance parameters." *Magn Reson Med,* Vol. 73 (No. 6), pp. 2174-84, Jun (2015).

25- Z. Wang, B. C. Vemuri, Y. Chen, and T. H. Mareci, "A constrained variational principle for direct estimation and smoothing of the diffusion tensor field from complex DWI." *IEEE Trans Med Imaging,* Vol. 23 (No. 8), pp. 930-9, Aug (2004).

26- C. G. Koay, J. D. Carew, A. L. Alexander, P. J. Basser, and M. E. Meyerand, "Investigation of anomalous estimates of tensor-derived quantities in diffusion tensor imaging." *Magn Reson Med,* Vol. 55 (No. 4), pp. 930-6, Apr (2006).

27- J. Nocedal, Numerical Optimization. *Springer New York*, (1999).

28- D. Tschumperle, "Variational frameworks for DT-MRI estimation, regularization and visualization." in *Proceedings Ninth IEEE International Conference on Computer Vision*, (2003), pp. 116-21.

29- M. Moakher, "A differential geometry approach to the geometric mean of symmetric positive-definite matrices." *SIAM J Matrix Analy Applicat,* pp. 734-47, (2005).

30- Xavier Pennec, Pierre Fillard, and Nicholas Ayache, "A Riemannian Framework for Tensor Computing." *International Journal of Computer Vision,* Vol. 66 (No. 1), pp. 41-66, 2006/01/01 (2006).

31- Arsigny V, "Fast and simple calculus on tensors in the Log-Euclidean framework." in *MICCAI*, (2005), pp. 115-22.

32- Y. Kong, Y. Li, J. Wu, and H. Shu, "Noise reduction of diffusion tensor images by sparse representation and dictionary learning." *Biomed Eng Online,* Vol. 15p. 5, Jan 13 (2016).

33- P. Fillard, X. Pennec, V. Arsigny, and N. Ayache, "Clinical DT-MRI estimation, smoothing, and fiber tracking with log-Euclidean metrics." *IEEE Trans Med Imaging,* Vol. 26 (No. 11), pp. 1472-82, Nov (2007).

34- Zhenhua Lin, Riemannian Geometry of Symmetric Positive Definite Matrices via Cholesky Decomposition. (2019).

35- J. D. Tournier, "Mrtrix3: A fast, flexible and open software framework for medical image processing and visualization." *Neuroimage,* pp. 116-37, (2019).

36- P. Cook and et al, "Camino: Open-source diffusion-MRI reconstruction and processing." in *14th Scientific Meeting and Exhibition*, (2006), pp. 27-59.

37- B. Geveci J. P. Ahrens, and C. C. Law, Paraview: An end-user tool for large-data visualization. (*The Visualization Handbook*). (2005).

38- A. Leemans, "ExploreDTI: a graphical toolbox for processing, analyzing, and visualizing diffusion MR data." (2009).

39- D. K. Jones, "White matter integrity, fiber count, and other fallacies: The do's and don'ts of diffusion MRI." *Neuroimage,* (2012).

40- J. Veraart, "A comprehensive framework for accurate diffusion MRI parameter estimation." *Magn Reson Med,* (2012).